EFFECT OF ELECTROPHORETIC DEPOSITION PARAMETERS ON COATING THICKNESS AND DEPOSIT YIELD OF NON-COLLOIDAL GRAPHITE PARTICLES

Kok-Tee Lau[a]*, C. C. Sorrell[b]

[a]Faculty of Industrial & Manufacturing Technology & Engineering, Universiti Teknikal Malaysia Melaka, Hang Tuah Jaya, 76100 Durian Tunggal, Melaka, Malaysia
[b]School of Materials Science and Engineering, UNSW Sydney, Australia

Graphical abstract
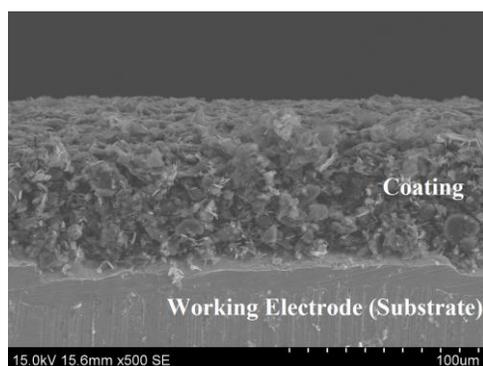
Abstract

Electrophoretic Deposition (EPD) has become a method for fabricating and enhancing electrodes for electrochemical energy storage (EES) devices. This article explores the impact of dominant EPD parameters on the deposit yield and coating thickness of graphite produced from an organic-based graphite particle suspension. The deposit yield follows a linear Hamaker's law at voltages below 50 V, with a deposition time of up to 5 minutes and solid loading between 2.5 to 12.5 mg/mL. The study also demonstrates the successful deposition of negatively charged and non-colloidal sized graphite particles, which are previously dispersed in n-butylamine-acetone without the use of charging or binding additives. This later forms a coating with a relatively strong binding strength of graphite particles on the steel anode. EPD of graphite suspension with a concentration of 5 mg/mL at a deposition voltage of 10 V and 5 minutes deposition time is capable of producing a graphite coating thickness of 70 μm. This research demonstrates the high-yield capability of EPD of organic-based graphite particles on metal anode and provides valuable insight for future investigations into application of binderless graphite suspension particles for electrode materials in energy storage systems.

Keywords: Lithium-ion batteries, supercapacitors, electrophoretic deposition, graphite, electrode materials

Abstrak

Pemendapan Elektroforetik (EPD) telah menjadi kaedah untuk membuat dan mempertingkatkan elektrod untuk peranti simpanan tenaga elektrokimia (EES). Artikel ini meneroka kesan parameter EPD dominan pada hasil deposit dan ketebalan salutan grafit yang dihasilkan daripada ampaian zarah grafit berasaskan organik. Hasil deposit mengikut hukum Hamaker linear pada voltan di bawah 50 V, dengan masa pemendapan sehingga 5 minit dan pemuatan pepejal antara 2.5 hingga 12.5 mg/mL. Kajian ini juga menunjukkan pemendapan yang berjaya bagi zarah grafit bercas negatif dan bersaiz bukan koloid, yang sebelum ini tersebar dalam n-butylamine-acetone tanpa menggunakan bahan tambahan pengecasan atau pengikat. Ini kemudiannya membentuk salutan dengan kekuatan

mengikat zarah grafit yang agak kuat pada anod keluli. EPD ampaian grafit dengan kepekatan 5 mg/mL pada voltan pemendapan 10 V dan masa pemendapan 5 minit mampu menghasilkan ketebalan salutan grafit 70 μm. Penyelidikan ini menunjukkan keupayaan hasil tinggi EPD bagi zarah grafit berasaskan organik pada anod logam dan memberikan pandangan yang berharga untuk penyiasatan masa depan ke dalam aplikasi zarah penggantungan grafit tanpa pengikat untuk bahan elektrod dalam sistem penyimpanan tenaga.

Kata kunci: Bateri litium-ion, supercapacitors, pemendapan elektroforesis, grafit, bahan elektrod

1.0 INTRODUCTION

Electrophoretic Deposition (EPD) has recently gained acceptance as a method for fabricating and enhancing electrodes for electrochemical energy storage (EES) devices [1, 2, 3]. Since 2010, the EPD method has been proposed as an alternative fabrication method for depositing electrode materials due to its simple setup, flexible control, and feasibility to be scaled up [4, 5]. Recently, the advantage of EPD in assembling high homogeneity 3D nanostructures and binder-free electrodes has been recognized as a better approach compared to other conventional methods to enhance the performance of EES electrodes [1]. Herein, electrode materials fabricated by EPD are superior to the conventional fabrication methods such as tape (slurry) casting and spin-coating methods in terms of their electrical and mechanical properties [2].

Recent papers on EPD of carbon materials demonstrates various ways to combine carbon nanotubes (CNTs) with carbon black and graphene particles to produce conductive electrode materials [1, 2, 6]. However, limited studies have been conducted on the effect of EPD parameters of graphite particles, particularly the organic (non-aqueous) suspension medium mixture formulation, on the properties of the deposited graphite electrode material [2]. The potential of graphite candidate as an EES electrode material is significant due to graphite's electrical conductivity, which is three times higher than that of copper [7, 8], and is cheaper than CNTs and graphene in terms of material cost. Furthermore, the performance of graphite electrode material has been proven in older generations of batteries and has been continuously used for ion batteries [9].

Previous studies had reported that it is difficult to perform the EPD of graphite particles from a pure suspension medium [10, 11, 12]. Graphite particles need to be suspended in a suspension medium either with the help of electrolyte additives (i.e. nitrate or phosphate salts) [10, 11, 13] or are steric-stabilized with the presence of polymer particulates [11, 14]. To the best of the authors' knowledge, the only reported study on EPD of graphite without the usage of additives was made by Lu *et al.* [15] as cited in Hajizadeh *et al.* [2], which used acetonitrile-triethylamine as a suspension medium. Since the organic mixture is environmentally harmful and has high toxicity, there is a need to find an alternative suspension medium that is more feasible for the EPD of the graphite electrode material.

This paper reports on the effect of various dominant EPD parameters on the deposit yield (i.e. mass per unit deposition area) and coating thickness of non-colloidal-sized graphite particle suspensions in the n-butylamine-acetone organic medium mixture. The EPD parameters examined include applied voltage, deposition time, solid loading (graphite particle concentration), and volume mixture ratio of the n-butylamine-acetone organic medium. Non-colloidal graphite particles with a size less than 20 μm are used in this study due to the low material cost and are easily deposited without the usage of charging or binding additives. It had been reported that the optimum particle size for electrophoretic deposition is normally in the range of 1-20 μm [16].

The current study found that a relatively stable negatively-charged graphite particle suspension can be formed in the n-butylamine-acetone organic medium in the absence of a charging agent, resulting in a successful deposition at a higher yield capability compared to previous studies [13, 15]. This study contributes to the understanding of EPD for graphite particle suspensions in n-butylamine-acetone organic media and provides valuable insight for future investigations into using graphite particles for electrode materials in EES.

2.0 METHODOLOGY

Unmodified synthetic graphite particles from Sigma-Aldrich (product number: 282863, 99.7 wt%) were used in this study. The morphology of these graphite particles, as illustrated in Figure 1, is sub-angular and of low sphericity based on the shape classification proposed by Powers [17], as cited in Maroof *et al.* [18], and many particles are in flake shape, indicating an exfoliation process has occurred. Figure 1 also shows that most particles are larger than 1 μm.

The graphite particles' datasheet from the supplier indicates that the particle size is less than 20 μm. According to Lyklema [19], colloidal particles dispersed in a medium have at least one dimension roughly between 1 nm and 1 μm. Since the graphite particles' size is more than 1 μm (i.e. non-colloidal size range) in diameter and the larger particles dictate the deposit yield, EPD behavior of these graphite particles is presumed to be non-colloidal in nature. Contrary to colloidal particles, which tend to stay in suspension for a long period due to Brownian motion, the non-colloidal particles require continuous hydrodynamic agitation to remain in suspension [16, 20].
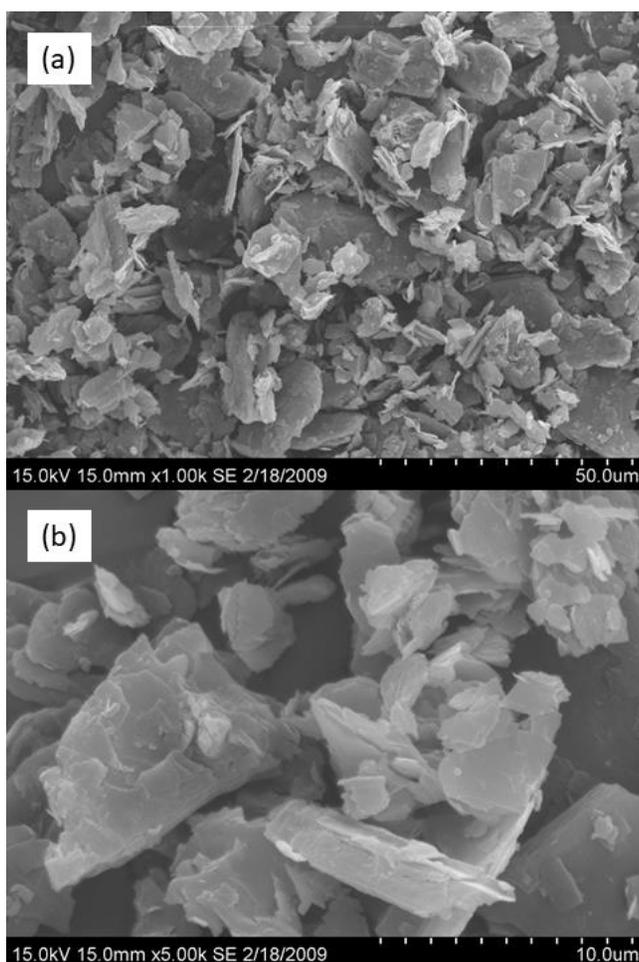
Figure 1 Microstructure of graphite particles in low (a) and high (b) magnifications

A suspension of 5.0 mg/mL graphite was prepared by adding 100 mg of as-received graphite particles to a 20 mL mixture of n-butylamine-acetone organic medium with a volume ratio of 2.5:7.5. Both the reagent-grade organic media were supplied by Sigma-Aldrich and have a purity of 99.5%. The suspension was magnetically stirred at a speed of 400 rpm for 1 minute using a 2 cm Teflon-coated bar in a 25 mL Pyrex beaker.

The anode, or working electrode, was a sheet of AISI-SAE-1006 grade low carbon steel (with dimensions of 10 mm H × 5 mm W × 0.55 mm T) while the cathode, or counter-electrode, was a sheet of AISI-SAE 304 grade stainless steel (with submerged dimensions of 10 mm H × 10 mm W × 1.5 mm T) from BlueScope Steel Ltd. Australia. Both electrodes were cleaned and dried before being connected to a programmable power supply (EC2000P, E-C Apparatus Corp., USA). The parallel distance between the electrodes was kept at 1 cm. After submerging the electrodes vertically into a freshly prepared suspension, the EPD process was performed at a constant voltage of 10-50 V for 1-5 minutes deposition time. To ensure the uniformity of the suspension and minimize the amount of particle settling during EPD, the suspension was agitated by magnetic stirring right before the EPD, and EPD time was set to short deposition time (i.e. 1, 2, 3, 4 and 5 minutes). The deposited sample was withdrawn carefully from the suspension after EPD, and then allowed to dry in the ambient environment for one day before being weighed. The deposit yield was determined by subtracting the weight of the deposited sample from the bare working electrode's weight measured before the EPD.

The microstructure of the as-received graphite particles and the deposited samples was studied using scanning electron microscopy (SEM, 15 kV accelerating voltage, secondary electron emission mode, S3400N, Hitachi High-Technologies Co., Japan). Contrary to the samples for surface microstructural observation, which were observed in as-deposited form, the coating covering the edges of samples for cross-section microstructural observation was carefully removed by a knife blade prior to the SEM observation for better image focus. The coating thickness and the corresponding error bar of each of the deposited samples were obtained from their cross-sectional micrographs using ImageJ software (version 1.42q).

The effect of EPD parameters (i.e. applied voltage, deposition time, graphite particles' solid loadings, and n-butylamine-acetone suspension medium volume ratio) on the deposit yield and formed thickness were investigated by varying only one of these parameters while keeping the others as constant.

3.0 RESULTS AND DISCUSSION

The plot of deposit yield as a function of applied voltage, graphite particles' solid loading (also known as concentration), and deposition time are explained by Hamaker's law. The Hamaker's law expresses the relationship between the deposit mass $m(t)$ and the EPD parameters [21] as:

$$m(t) = \int_0^t f \cdot M_E \cdot A \cdot c(t) \cdot E(t) \cdot dt \qquad (1)$$

where
t is deposit time in s,
f is the unitless efficiency factor ($0 \leq f \leq 1$; $f = 1$ if all particles that reached the substrate are deposited),
M_E is the electrophoretic mobility in μm^2/V.s,
A is the deposited surface area in cm^2,
$c(t)$ is the particle mass concentration in grams and
$E(t)$ is the applied electric field in V/cm.

In this study, the deposit yield (d.y.) in mg/cm^2 is calculated by dividing the measured weights of the deposited graphite particles, $m(t)$ by the deposited surface area, A. Since the anode-cathode separation (also known as distance) L was maintained constant at 1 cm for characterization purposes, the applied voltage was equivalent to the electric field generated between the anode and cathode. Thus, a modified Hamaker's expression can be written as follow:

$$d.y.(t) = \int_0^t f \cdot M_E \cdot c(t) \cdot \frac{V(t)}{L} \cdot dt \qquad (2)$$

When the EPD parameters mentioned above (except for the applied voltage) were fixed, a graph of the deposit yield as a function of voltage (Figure 2) was obtained. The deposit yield data on the anode plate (working electrode) were measured in three ways: (I) deposit yield on both sides (front and back sides), (II) deposit yield on the front side (anode side facing cathode), and (III) deposit yield on the back side (anode side facing away from cathode). The graph of coating thickness of the anode's front side deposit is also provided to show the dimensional characteristics of the formed deposit as a function of voltage.

The deposit yield versus voltage behavior of the Front and Back side coatings is similar. This result implies that the deposit yield on both sides of the formed coating behaves similarly as electrophoretic deposition was performed. When comparing deposition yield at a low voltage (10 V), the difference between the deposit yield of the Front and Back sides becomes less significant.

A benchmarking comparison of the graphite deposit yield demonstrates that the current non-colloidal graphite suspension is able to produce two times the yield of Das *et al.* [13] at the voltage between 50 V and 150 V when deposited for 5 minutes, although no charging additive is used in the current study as compared to Das *et al.* study. In another study, Lu *et al.* [15] showed that deposition of graphite particles without a charging additive at 24 V for 15 minutes only managed to produce a deposit yield of less than 0.1 mg for an electrode diameter of 1.43 cm (i.e. less than 0.07 mg/cm^2 yield) after undergoing two deposition cycles.

As the voltage increases beyond 50 V, the deposit yield increase rate starts to decrease logarithmically with increasing voltage, demonstrating a divergence from a linear Hamaker's law relationship. A recent simulation study by Salazar *et al.* [22] demonstrated

that the reason for the nonlinear yield growth is caused by the depletion of suspended particles in the vicinity of the depositing electrode when deposition occurs at high applied voltage and long deposition time. As the electric field pushes the particles toward the depositing electrode, a region devoid of particles develops due to mass conservation. The particle depletion happens because there is no flow of new particles coming from the counter electrode.
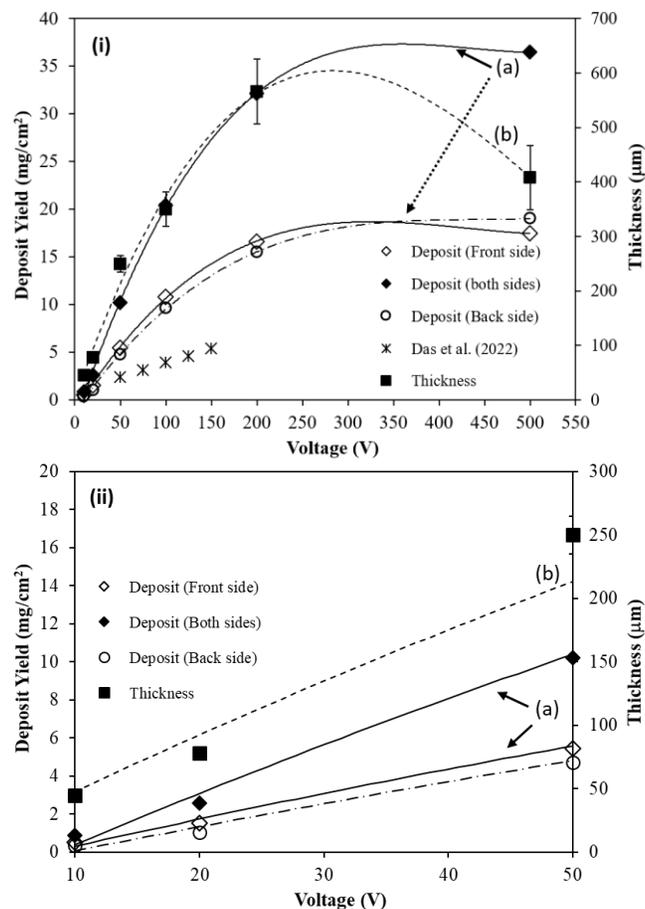
Figure 2 (i) Deposit yield versus voltage of graphite coating from the current study (labelled as (a)) and Das *et al.* [13], as well as thickness of the front side coating (labelled as (b)), and (ii) the enlargement of the graph at 10-50 V range (Deposition time = 5 minutes, graphite solids loading = 5 mg/mL, n-butylamine-acetone ratio = 2.5:7.5)

The cross-sectional study, illustrated by Figure 3, shows that an uneven coating thickness is formed, with thicker coating observed at the edges of the working electrode. Figure 2 shows that the deposit thickness increases with the voltage's increase but decreases after the voltage exceeds 200 V. It is also important to note that the thickness variation (represented by the data's error bar) becomes apparent after 50 V, and the thickness variation increases with voltage from 50 V until 500 V. A previous study showed that the electric field density is higher at the electrode edges than in the planar

region [23]. A higher electric field density means graphite particles experience a stronger electric force directed toward the electrode edges. This explains a higher deposit yield rate throughout the deposition process, creating a thicker coating morphology at the electrode edges. Regarding the decrease of measured coating thickness (as shown by graph (b) of Figure 2(i)) compared to the plateau behavior shown by the deposit yield, the mismatched behavior was exacerbated by the mechanical removal of thick and uneven coating grown along the electrode's edges when preparing for SEM cross-sectional observation (as mentioned earlier in the Methodology section).
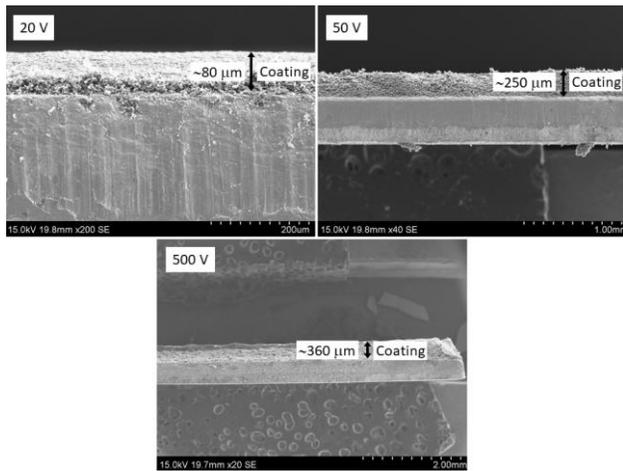
Figure 3 SEM micrographs of the cross-sectional microstructures of graphite coating deposited at different voltages

The deposition kinetics of the graphite particles deposition is conducted by investigating the deposition yield versus deposition time (Figure 4). After a deposition time of 1 minute, a patchy deposit is formed on the depositing electrode (Figure 5). Since there is no continuous coating layer for deposition of 1 minute, thickness measurement was not performed.

A continuous coating is formed for a deposition time of 2 minutes and longer. Still, the deposition surface shows a wavy microstructure because the permanent bonding of particles onto the electrode is initiated by the particle-agglomeration. Lau *et al.* had suggested that the particle-agglomeration-driven deposition governs the deposition mechanism of particles [24]. Particle-agglomeration-driven deposition can be explained by either one of the four well-known deposition mechanisms as reported recently [2]:

1. Flocculation by particle accumulation,
2. Particle charge neutralization,
3. Electrochemical particle coagulation, or
4. Electrical double layer (EDL) distortion and thinning
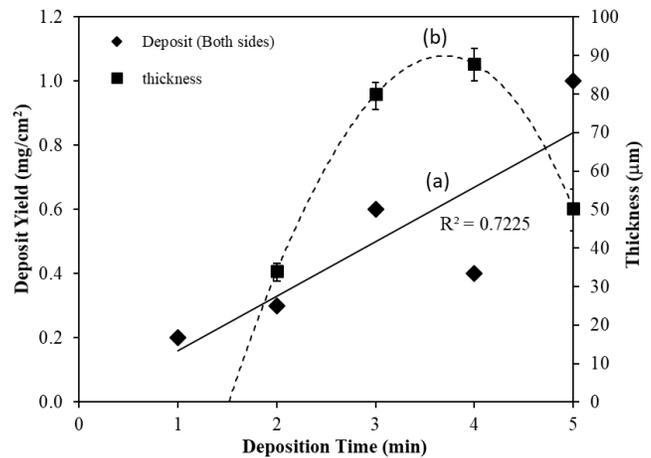
Figure 4 (a) Deposit yield of graphite coating on both sides of the working electrode, and (b) coating thickness (front side), as function of deposition time (Applied voltage = 10 V, graphite solids loading = 5 mg/mL, n-butylamine-acetone ratio = 2:8)
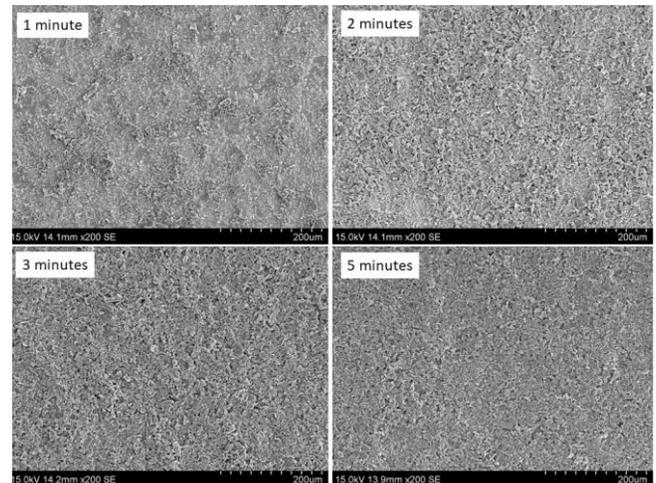
Figure 5 SEM micrographs of the surface microstructures of graphite coating deposited at different deposition times

The coating thickness versus deposition time exhibits a quadratic behavior, where there is a thickness reduction after the deposition time exceeds 4 minutes. The trend is confirmed by the cross-sectional microstructural study of the coating (see Figure 6). However, the deposit yield data versus deposition time shows that the deposit yield increases linearly until 5 minutes of deposition time. Similar to Figure 2(i), the discrepancy between the thickness and deposit yield data of Figure 6 shows that the thickness data is more sensitive than the deposit yield data towards external factors such as non-uniform electric field generation by the anode during EPD and the subsequent SEM sample preparation process.
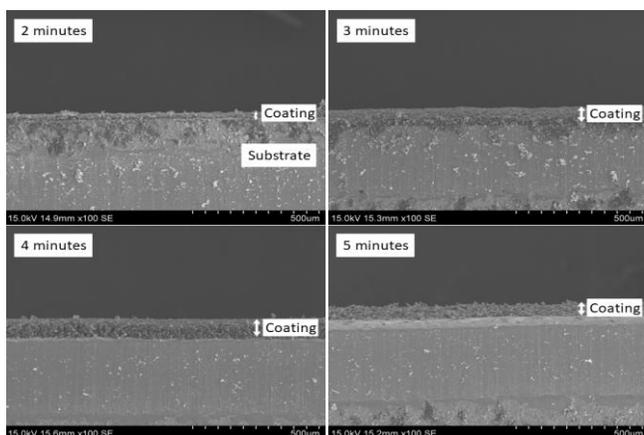
Figure 6 SEM micrographs of the cross-sectional microstructures of graphite coating deposited at different deposition times

Mohanty *et al*. [25] and Wang *et al*. [26], as cited in Hajizadeh *et al*. [2], reported that when particle concentration is not conserved over time, the concentration factor becomes a predominant factor compared to the voltage factor. However, our findings (refer to Figure 7) show that the applied voltage factor has more influence than the concentration (solid loading) factor in increasing deposit yield. For example, an order of magnitude increase in solid loading (from 2.5 mg/mL to 12.5 mg/mL) only generates a 207% and 253% increase in deposit yield at 10 V and 100 V, respectively. In contrast, the same order of magnitude increase in voltage (from 10 V to 100 V) produces about a 2000% to 2585% increase in deposit yield. EPD mechanisms, as reported by Hajizadeh *et al*. [2], involve interparticle interaction, which is related directly to the interparticle distance during the EPD process. It is believed that the graphite suspension's concentration used in the current study is nearly saturated, and the highly concentrated suspension caused the sedimentation rate of graphite particles, especially the non-colloidal-size, to grow. The inhibiting factor results in a slight deposit yield increment as the solids loading rises.
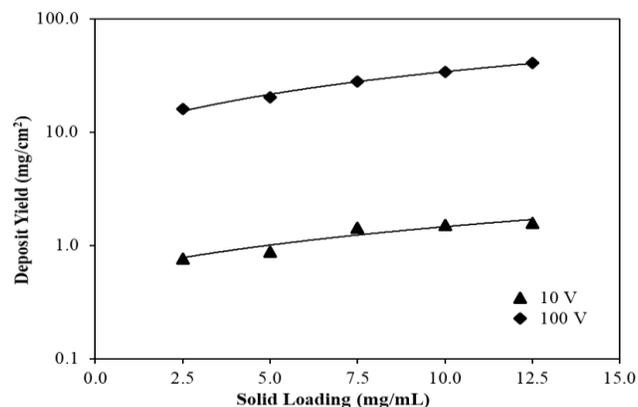
Figure 7 Deposit yield versus graphite particles' solid loading for the deposition voltage of 10 V and 100 V (deposition time = 5 minutes, n-butylamine-acetone ratio = 2.5:7.5)

Meanwhile, previous studies on the effect of n-butylamine:acetone medium formulation on the electrophoretic deposition of carbon-based particles have been very rare [27]. Figure 8 shows the deposit yields obtained using graphite suspension in different n-butylamine-acetone composition ratios shows a linear Hamaker's relationship with the increasing deposition time. The data is verified by the surface microstructure study (see Figure 9). However, the deposit yield difference between the coating samples is very small, with a weight difference of about 0.2 mg at a deposition time of 3 minutes when the n-butylamine concentration varies from 15 vol% to 25 vol% of the total medium volume. The difference may be due to the low voltage and deposition time.

The deposit yield increment variation with different n-butylamine-acetone composition ratios indicates the implication of the latter to the electrophoretic mobility of graphite suspension particles. Graphite particles are expected to have an acidic surface, and the mixture of acetone and n-butylamine is a basic medium [28]. Thus, the resulting acid-basic reaction causes electron transfer from the n-butylamine-acetone medium to the surface of the graphite particles. Labib and Williams [29, 30], as cited in Van der Biest and Vandeperre [31], had proposed electron exchange as the charging mechanism of particles in this non-aqueous (organic) media. The effect of electron transfer mechanism from n-butylamine to graphite and graphene layers had been demonstrated in the recent studies [8, 32].

It is also observed that the deposit yield after 3 minutes deposition time is the highest when the n-butylamine volume is the highest (refer to Figure 8). The introduction of the basic amine group of n-butylamine enhances the basicity of the acetonic suspension medium, thus raising the ionic concentration in the suspension medium [27]. Furthermore, the lone pair electrons of n-butylamine molecules interact with the surface of graphite particles (the mechanism is illustrated in Figure 10). Graphite has defects and edges [33] where the amine group of n-butylamine molecules can attach, which can lead to electron transfer from n-butylamine to the graphite particles' surface. After the electron transfer, graphite particles become increasingly negatively charged, and the electrophoretic mobility of the graphite particles increases. Consequently, the deposit yield of the graphite particles is also increased.

Considering the difficulties in measuring the zeta potential (the derivation of electrophoretic mobility) in n-butylamine-acetone and that the results obtained are not as accurate as in water, the possibility of using the suspension in as-prepared condition was also an advantage because there was no need to adjust the zeta potential by adding acid. The graphite coatings were always deposited on the positive electrode irrespective of the EPD parameters; this further confirms the negative charge

of the graphite particles in the acetone-n-butylamine suspension medium. Negative carbon-based particles were also obtained by a previous study when suspended in the acetone-n-butylamine suspension medium [28].
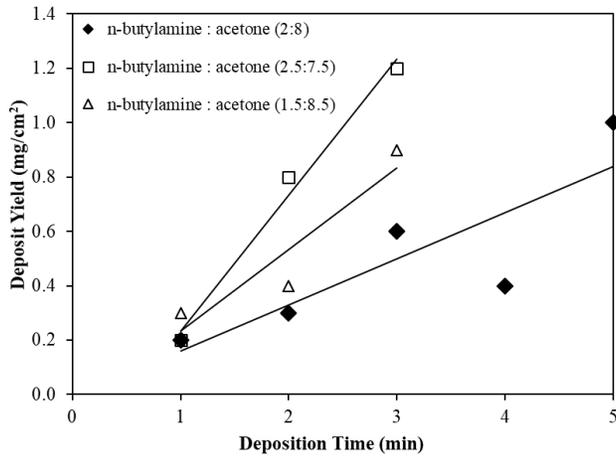
Figure 8 Deposit yield as a function of deposition time for the deposition of graphite particles in different n-butylamine:acetone medium ratios (applied voltage = 10 V, graphite solids loading = 5 mg/mL)
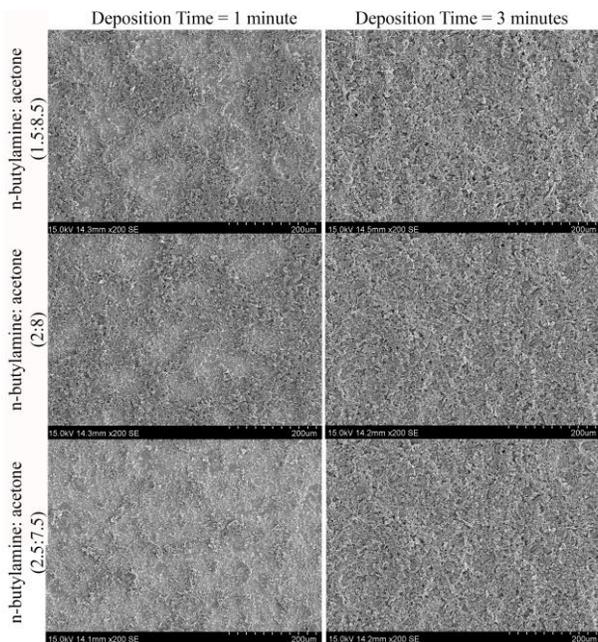
Figure 9 SEM micrographs of the surface microstructures of graphite coating deposited using different n-butylamine-acetone ratios, after 1 minute and 3 minutes of deposition
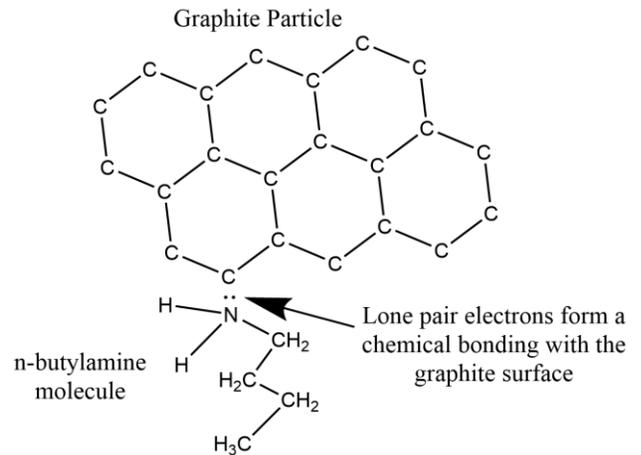
Figure 10 Schematic diagram of a n-butylamine molecule interacting through its lone pair electrons with the surface of a graphite particle

4.0 CONCLUSION

This study specifically investigated the impact of several dominant EPD parameters on the deposit yield and coating thickness of organic-based graphite particle suspensions. Overall, this research advances the understanding of EPD for graphite particle suspensions in an organic medium and provides valuable insight for future investigations into the electrophoretic deposition of organic-based graphite particles on a metal anode for electrode materials in energy storage systems. For future work, we recommend extending the study of n-butylamine:acetone-based EPD to other carbon materials such as CNTs, graphene, or a combination of the carbon-based particles. Additionally, the characterization of the EPD coating should be expanded to include specific capacity and power density performance for application in energy storage systems (EES).

Conflicts of Interest

The author(s) declare(s) that there is no conflict of interest regarding the publication of this paper.

Acknowledgement

References

[1] Chakrabarti, B. K., M. Gençten, G. Bree, A. H. Dao, D. Mandler, and C. T. J. Low. 2022. Modern Practices in Electrophoretic Deposition to Manufacture Energy Storage Electrodes. *International Journal of Energy Research*. 46(10): 13205-13250. Doi: https://doi.org/10.1002/er.8103.

[2] Hajizadeh, A., Taieb S., Reza R., Maziar S. Y., Babak R., Saleh G., Alireza A., Sepideh R. and Aliasghar S. G. 2022. Electrophoretic Deposition as a Fabrication Method for Li-ion Battery Electrodes and Separators – A Review. *Journal of Power Sources*. 535: 231448. Doi: https://doi.org/10.1016/j.jpowsour.2022.231448.

[3] Hu, S., Li, W., Finklea, H., and Liu, X. 2020. A Review of Electrophoretic Deposition of Metal Oxides and Its Application in Solid Oxide Fuel Cells. *Advances in Colloid and Interface Science*. 276: 102102. Doi: https://doi.org/10.1016/j.cis.2020.102102.

[4] Lau, K. -T., Azam, M. A., and Seman, R. N. A. R. 2018. Influence of Pulsed Electrophoretic Deposition of Graphitic Carbon Nanotube on Electrochemical Capacitor Performance. *Journal of Engineering Science and Technology*. 13(2): 295-308.

[5] Talib, E., Lau, K. -T., Zaimi, M., Bistamam, M. S. A., Manaf, N. S. A., Seman, R. N. A. R., Zulkapli, N. N., and Azam, M. A. 2015. Electrochemical Performance of Multi Walled Carbon Nanotube and Graphene Composite Films Using Electrophoretic Deposition Technique. *Applied Mechanics and Materials*. 761: 468-472.

[6] Rehman, M. A. U., Chen, Q., Braem, A., Shaffer, M. S. P., and Boccaccini, A. R. 2021. Electrophoretic Deposition of Carbon Nanotubes: Recent Progress and Remaining Challenges. *International Materials Reviews*. 66(8): 533-562. Doi: https://doi.org/10.1080/09506608.2020.1831299.

[7] Pietronero, L., Strässler, S., Zeller, H. R., and Rice, M. J. 1980. Electrical Conductivity of a Graphite Layer. *Physical Review B*. 22(2): 904-910. Doi: https://doi.org/10.1103/PhysRevB.22.904.

[8] Yang, T. -C., Jiang, Y. -P., Lin, T.-H., Chen, S .-H., Ho, C. -M., Wu, M. -C., and Wang, J. -C. 2021. N-butylamine-modified Graphite Nanoflakes Blended in Ferroelectric P(VDF-TrFE) Copolymers for Piezoelectric Nanogenerators with High Power Generation Efficiency. *European Polymer Journal*. 159: 110754. Doi: https://doi.org/10.1016/j.eurpolymj.2021.110754.

[9] Yu, J., Lin, M., Tan, Q., and Li, J. 2021. High-value Utilization of Graphite Electrodes in Spent Lithium-ion Batteries: From 3D Waste Graphite to 2D Graphene Oxide. *Journal of Hazardous Materials*. 401: 123715. Doi: https://doi.org/10.1016/j.jhazmat.2020.123715.

[10] Arun, S., Hariprasad, S., Saikiran, A., Ravisankar, B., Parfenov, E. V., Mukaeva, V. R., and Rameshbabu, N. 2019. The Effect of Graphite Particle Size on the Corrosion and Wear Behaviour of the PEO-EPD Coating Fabricated on Commercially Pure Zirconium. *Surface and Coatings Technology*. 363: 301-313. Doi: https://doi.org/10.1016/j.surfcoat.2019.02.033.

[11] Fiołek, A., Zimowski, S., Kopia, A., Łukaszczyk, A., and Moskalewicz, T. 2020. Electrophoretic Co-deposition of Polyetheretherketone and Graphite Particles: Microstructure, Electrochemical Corrosion Resistance, and Coating Adhesion to a Titanium Alloy. *Materials*. 13(15): 3251. Doi: https://doi.org/10.3390/MA13153251.

[12] Liao, Y., Cao, L., Wang, Q., Li, S., Lin, Z., Li, W., Zhang, P., and Yu, C. 2022. Enhanced Tribological Properties of PEEK-based Composite Coatings Reinforced by PTFE and Graphite. *Journal of Applied Polymer Science*. 139(13): e51878. Doi: https://doi.org/10.1002/app.51878.

[13] Das, D., Majumder, S. B., Dhar, A., and Basu, S. 2022. Electrophoretic Deposition: An Attractive Approach to Fabricate Graphite Anode for Flexible Li-Ion Rechargeable Cells. *Journal of Materials Science: Materials in Electronics*. 33(16): 13110-13123. Doi: https://doi.org/10.1007/s10854-022-08250-5.

[14] Ma, J., Wang, C., and Liang, C. H. 2007. Colloidal and Electrophoretic Behavior of Polymer Particulates in Suspension. *Materials Science and Engineering C*. 27(4): 886-889. Doi: https://doi.org/10.1016/j.msec.2006.10.005.

[15] Lu, Y., Zhang, D., Wang, L., Xu, M., Song, J., and Goodenough, J. B. 2012. Electrochemical Behavior of a Graphite Electrode Prepared by Anodic Electrophoretic Deposition. *Journal of The Electrochemical Society*. 159(3): A321. Doi: https://doi.org/10.1149/2.078203jes.

[16] Heavens, S. N. 1990. Electrophoretic Deposition as a Processing Route for Ceramics. In J. G. P. Binner (ed.) *Advanced Ceramic Processing and Technology*. Park Ridge, USA: Noyers Publications.

[17] Powers, M. C. 1953. A New Roundness Scale for Sedimentary Particles. *Journal of Sedimentary Research*. 23(2): 117-119.

[18] Maroof, M. A., Mahboubi, A., Noorzad, A., and Safi, Y. 2020. A New Approach to Particle Shape Classification of Granular Materials. *Transportation Geotechnics*. 22: 100296. Doi: https://doi.org/10.1016/j.trgeo.2019.100296.

[19] Lyklema, J. 2005. *Fundamentals of Interface and Colloid Science: Particulate Colloids*. Vol. IV. Amsterdam, Netherlands: Elsevier Academic Press.

[20] Besra, L., and Liu, M. 2007. A Review on Fundamentals and Applications of Electrophoretic Deposition (EPD). *Progress in Materials Science*. 52(1): 1-61. Doi: https://doi.org/10.1016/j.pmatsci.2006.07.001.

[21] Kinzl, M., Reichmann, K., and Andrejs, L. 2009. Electrophoretic Deposition of Silver from Organic PDADMAC-stabilized Suspensions. *Journal of Materials Science*. 44(14): 3758-3763. Doi: http://dx.doi.org/10.1007/s10853-009-3504-x.

[22] Salazar de Troya, M. A., Morales, J. R., Giera, B., Pascall, A. J., Worsley, M. A., Landingham, R., Du Frane, W. L., and Kuntz, J. D. 2021. Modeling Flow-based Electrophoretic Deposition for Functionally Graded Materials. *Materials & Design*. 209: 110000. Doi: https://doi.org/10.1016/j.matdes.2021.110000.

[23] Pascall, A. J., Sullivan, K. T., and Kuntz, J. D. 2013. Morphology of Electrophoretically Deposited Films on Electrode Strips. *The Journal of Physical Chemistry B*. 117 (6): 1702-1707. Doi: https://doi.org/10.1021/jp306447n.

[24] Lau, K. -T., and Samsudin, S. 2022. Electrophoretic Deposition of Hexagonal Boron Nitride Particles from Low Conductivity Suspension. *Journal of Science and Technology*. 30(2): 1237-1256. Doi: https://doi.org/10.47836/pjst.30.2.21.

[25] Mohanty, G., Besra, L., Bhattacharjee, S., and Singh, B. P. 2008. Optimization of Electrophoretic Deposition of Alumina onto Steel Substrates from its Suspension in Iso-propanol using Statistical Design of Experiments. *Materials Research Bulletin*. 43(7): 1814-1828. Doi: https://doi.org/10.1016/j.materresbull.2007.07.014.

[26] Wang, Y. -Q., Byun, J. -H., Kim, B. -S., Song, J. -I., and Chou, T. -W. 2012. The Use of Taguchi Optimization in Determining Optimum Electrophoretic Conditions for the Deposition of Carbon Nanofiber on Carbon Fibers for Use in Carbon/epoxy Composites. *Carbon*. 50(8): 2853-2859. Doi: https://doi.org/10.1016/j.carbon.2012.02.052.

[27] Vandeperre, L., and Van Der Biest, O. 1997. Influence of Iso-propyl Alcohol Addition on the Electrophoretic Deposition of SiC from a Mixture of Acetone and n-butylamine. *Key Engineering Materials*. 132-136: 293-296.

[28] Vandeperre, L., Van Der Biest, O., Bouyer, F., Persello, J., and Foissy, A. 1997. Electrophoretic Forming of Silicon Carbide Ceramics. *Journal of the European Ceramic Society*. 17(2-3): 373-376. Doi: https://doi.org/10.1016/s0955-2219(96)00106-9.

[29] Labib, M. E., and Williams, R. 1984. The Use of Zeta-potential Measurements in Organic Solvents to Determine the Donor-acceptor Properties of Solid Surfaces. *Journal of*

Colloid and Interface Science. 97(2): 356-366. Doi: https://doi.org/10.1016/0021-9797(84)90306-0.

[30] Labib, M. E., and Williams, R. 1986. An Experimental Comparison between the Aqueous pH Scale and the Electron Donicity Scale. *Colloid & Polymer Science*. 264(6): 533-541. Doi: https://doi.org/10.1007/BF01422007.

[31] Van der Biest, O. O, and Vandeperre, L. J. 1999. Electrophoretic Deposition of Materials. *Annual Review of Materials Science*. 29(1): 327-352. Doi: https://doi.org/10.1146/annurev.matsci.29.1.327.

[32] Gholami, J., Manteghian, M., Badiei, A., Ueda, H., and Javanbakht, M. 2016. N-butylamine Functionalized Graphene Oxide for Detection of Iron(III) by Photoluminescence Quenching. *Luminescence*. 31(1): 229-235. Doi: https://doi.org/10.1002/bio.2950.

[33] An, S. J., Li, J., Daniel, C., and Wood, D. L. 2019. Effects of Ultraviolet Light Treatment in Ambient Air on Lithium-ion Battery Graphite and PVDF Binder. *Journal of the Electrochemical Society*. 166(6): A1121. Doi: https://doi.org/10.1149/2.0591906jes.